AIAA JOURNAL
Vol. 43, No. 11, November 2005

# Optimum Loading of a Tension Kite

Peter S. Jackson*
*University of Auckland, Auckland 1, New Zealand*

**A theory is presented for the optimum shape of tension kites based on lifting-line theory combined with the requirement that the kite shape and tension be in equilibrium everywhere with the forces normal to it. The flying shape of the kite then emerges as part of the solution, along with the distribution of twist, which must be built into any particular kite to achieve the required loading. Results are presented first for a kite in ideal flow, when all the important parameters scale with the lift coefficient, and then for a kite of realistic shape and profile drag.**

## Nomenclature

| | | |
|---|---|---|
| $A$ | = | reference area (e.g., top surface of the kite) |
| $b$ | = | kite span, or arc length of lifting line |
| $C_D, C_L, C_T$ | = | force coefficients based on $\frac{1}{2}\rho A U^2$ |
| $D, L$ | = | aerodynamic drag and lift |
| $s$ | = | distance along kite from centerline |
| $T$ | = | tension in each of two kite lines |
| $t, \phi$ | = | nondimensional measures of distance from centerline |
| $u, v, w$ | = | induced speeds |
| $v_n$ | = | induced speed in the kite plane, normal to kite and to $U$ |
| $x, y, z$ | = | coordinate axes |
| $\alpha_{\text{eff}}$ | = | effective angle of attack, $\alpha_g - \alpha_i$ |
| $\alpha_g$ | = | total geometric angle of attack, $\alpha_t + \alpha_k$ |
| $\alpha_i$ | = | induced angle of attack |
| $\alpha_k$ | = | incidence due to inclination $\varepsilon$ of the kite plane |
| $\alpha_t$ | = | incidence due to twist, measured from zero-lift angle |
| $\Gamma(s)$ | = | circulation of the kite at span $s$ |
| $\gamma(s)$ | = | wake vortex sheet strength at span $s$ |
| $\varepsilon$ | = | drag angle and flying angle of the kite |
| $\theta(s)$ | = | slope of the kite in its own plane |
| $\Lambda$ | = | aspect ratio, $b^2/A$ |
| $\rho, U$ | = | density and speed of incident flow |

## Introduction

A POPULAR kite design used in the sport of kite-surfing uses a self-inflating double-skin membrane section that is supported only by lines at the two ends so that the kite deforms into an arc when flying, as shown in Fig. 1. The idea of using a double-skin membrane has been highly developed in parafoils, but in that case there are many more lines to which the lift is transferred so that the lifting surface is flatter and produces more lift. The two-line kite must have a constant net spanwise tension which is transferred into the kite lines, and the action of this tension with the kite curvature must be in equilibrium with that part of the local load on the kite that is normal to the axis of curvature. Obviously the kite shape then depends on the kite loading and vice versa.

This raises the question of what the ideal distribution of loading along the span of such a kite must be. The ends of the kite must remain vertical, or nearly so, because they connect smoothly with the kite lines there. If the incidence of the kite section is increased toward the ends of the kite, then the kite will tend to open up so that the center is flatter and the kite will produce more lift. However, unless the induced angle is properly adjusted, this will at the same time produce more induced drag in a part of the kite that produces no useful lift, so that for a given net lift there must be an optimum loading distribution and an associated optimum kite shape. This question is resolved in the following by making use of lifting-line theory, which also turns out to be convenient in generating the solution of the kite shape.

There has been little work published on the aerodynamics of kites as such; most previous authors were concerned with kite stability or the loads on the kite tether. The paper by Alexander and Stevenson[1] provides a recent summary. However, membrane wings have been studied in much more detail, with various models being used for the structural support of the membrane. Early work concentrated on analytical models of two-dimensional sections in inviscid flow, and this work is summarized in the review by Newman.[2] Subsequent work, for example, that by Smith and Shyy[3] and Jackson and Fiddes,[4] has focused mainly on the addition of viscous effects using numerical methods. For three-dimensional membrane wings, the nonlinear behavior of shallow membrane structures and the coupling between the structural and the aerodynamic responses means that there can be no general analytical solution, even in inviscid flow. Progress may only be made for wings of particular kinds by making simplifying assumptions. It has been common,[5–9] for example, to assume that the membrane tension runs only in the chordwise direction when the addition of a cable along the trailing edge forms a tractable structural model. Solutions have also been obtained for cases where it can be assumed that the membrane is highly pretensioned.[10,11] However, except in a few special cases, none of these models have direct application to real membrane wings.

Letcher[12] made a significant contribution by showing that the structural analysis is greatly simplified if the membrane has a developable surface. This idea was developed by Sugimoto,[13] who developed a semi-analytical method for wings of cylindrical shape that are restrained only at the straight leading edge and at the center of the trailing edge. Subsequently Jackson[14] obtained solutions for wings composed of a conical surface that is restrained along the swept leading edges and the centerline. Although the assumption of a developable surface is still quite severe, in other respects these two models are close to the membrane wing configurations that are in common use as yacht sails and hang gliders. The present paper is a logical progression to wings that are supported only by tension in the spanwise direction, which once more is a reasonable representation of the structural behavior of the actual wings in question.

If the weight of the kite and lines is small compared to the aerodynamic forces on the kite, the requirements for equilibrium are quite straightforward and are illustrated in Fig. 2a. The kite at the point K is constrained by the line tension $2T$ (there being two lines here) to the ground at point G, the drag $D$ is aligned along the direction of the incident wind, and the lift $L$ is normal to the wind and lies in the plane of both the line and the drag. If there are two kite lines, as here, the kite may be flown stably at any azimuth angle $\psi$ without changing the attitude of the kite relative to the wind except for a solid-body rotation, and so the lift and drag remain unchanged. It

Received 2 July 2003; revision received 3 May 2005; accepted for publication 10 May 2005. 

*Professor, Department of Mechanical Engineering; currently Professor, College of Engineering, University of Canterbury, Christchurch, New Zealand. Member AIAA.

**Fig. 1a Tension kite in use.**

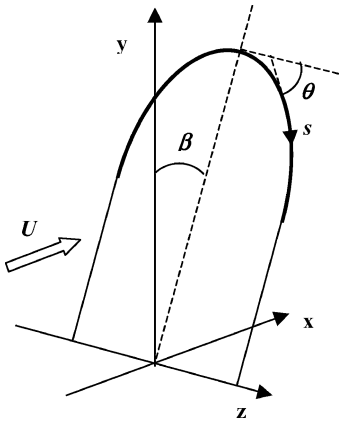


**Fig. 1b Flexible lifting-line geometry.**

follows that the flying angle $\varepsilon$ and tension are given by

$$\tan\varepsilon = D/L \tag{1a}$$

$$4T^2 = L^2 + D^2 \tag{1b}$$

and the effect of the azimuth angle $\psi$ is just to change the horizontal component of the lift: $L_H = L\cos\psi$.

These kites are used to propel vessels and vehicles (commonly buggies and kite-surfers) and so we must also consider their equilibrium. Figure 2b shows the balance of forces in a horizontal plane on a vessel proceeding at a true angle $\beta_T$ at speed $V_S$ into a wind of true speed $V_T$. The true speed is the wind speed at the height of the kite and the resulting apparent wind $V_A$ is the incident speed that the kite sees; the apparent angle $\beta_A$ determines the direction of the kite forces $D$ and $L_H$. The vessel produces side force and resistance forces, $S$ and $R$, whose directions are determined by the direction of its velocity $V_S$. As first shown by Lanchester (see Ref. 15), one condition for equilibrium of these forces is $\beta_A = \varepsilon_v + \varepsilon_A$, where $\tan\varepsilon_v = S/R$ and $\tan\varepsilon_A = D/L_H = \tan\varepsilon/\cos\psi$. Because higher vehicle speeds imply smaller values of the apparent angle, the drag angles of the vehicle and kite play a key role in determining the overall speed performance of the vessel.

If $\varepsilon_v \ll \varepsilon_A$, as with an iceboat, then maximum speed is achieved by minimizing the drag angle of the kite, but for other vessels it is usually not possible to minimize the two drag angles independently. For many waterborne vehicles, $\varepsilon_v$ dominates because the water resistance $R$ is so large, and to reduce this drag angle it may be best to deliberately increase the sideforce $S$: in that case the best kite may be that which has maximum lift, rather than the kite with the smallest drag angle. We must also note that the vertical component of kite lift

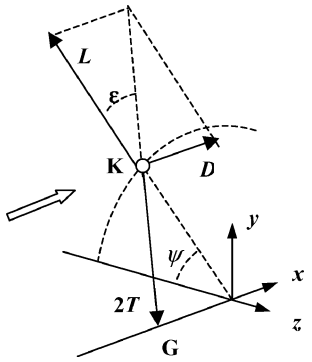


**Fig. 2a Equilibrium of kite forces.**

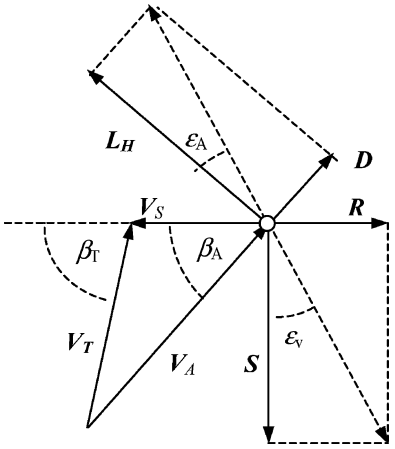


**Fig. 2b Balance of horizontal forces on a wind-driven vehicle.**

reduces the effective vehicle weight, and hence its resistance, and so the flying height of the kite also affects performance: that is, for a given kite and vehicle there must also be an optimum azimuth angle $\psi$. However, this interaction will be the subject of another paper, and here we simply note that for a given line tension or horizontal lift the aerodynamic driving force will be greatest when the kite drag is least. Because the angle $\psi$ is arbitrary this is equivalent to minimizing the kite drag for a given lift, and this needs to be done only for the special case $\psi = \pi/2$ when the lift force is vertical. In other cases the kite undergoes solid-body rotation to the appropriate value of $\psi$ while preserving the same spanwise distribution of lift.

## Aerodynamic Forces and Kite Equilibrium

The lifting surface of the kite is modeled using a lifting line bent into an arc, as shown in Fig. 1b. To define the geometry of the lifting line, we use a right-handed $x, y, z$ system as shown. With the kite and its lines initially lying in the $y$–$z$ plane, with the incident flow $U$ in the $x$ direction, the kite shape is defined by the arc length $s$ from the center of the line and the slope $\theta(s)$ of the line relative to the $z$ axis (positive downward). The kite plane is then rotated through an angle $\varepsilon$ about the $z$ axis, when the line tangent to the kite has components $\boldsymbol{i}_S = (-\sin\varepsilon\sin\theta, -\cos\varepsilon\sin\theta, \cos\theta)$.

According to the usual lifting-line assumptions, the wake is presumed to trail in the direction of the incident flow, so that it only induces velocities that are normal to this direction. The line itself induces further velocities which are normal to the plane in which it lies and so the $(x, y, z)$ components of the velocity at the line are written as $(U-u, -v, -w)$, where $u$, $v$, and $w$ are the (positive) self-induced terms, for which we may immediately make the usual assumption $u \ll U$. If the lifting line has a circulation $\Gamma(s)$ then, using the Kutta–Joukowsky theorem, the elemental lift and drag on a section d$s$ are

$$\mathrm{d}L = \rho(U\cos\theta - w\sin\theta\sin\varepsilon)\Gamma\,\mathrm{d}s$$

$$\mathrm{d}D = \rho(v\cos\theta + w\sin\theta\cos\varepsilon)\Gamma\,\mathrm{d}s$$

After integrating these elemental forces, Eq. (1a) reduces to

$$\sin\varepsilon U\int_{-b/2}^{b/2}\Gamma\cos\theta\,\mathrm{d}s=\int_{-b/2}^{b/2}\Gamma(v\cos\theta\cos\varepsilon+w\sin\theta)\,\mathrm{d}s \quad (2)$$

This provides the helpful insight that the angle $\varepsilon$ must be of the same order of magnitude as the induced angle of attack. Using Eq. (2), the net lift in the $y$ direction becomes

$$L=\rho\int\Gamma\cos\vartheta\,(U\cos^2\varepsilon+v\sin\varepsilon\cos\varepsilon)\,\mathrm{d}s$$

Consider now the overall force equilibrium of the kite in its own plane. The net flow normal to this plane is $u_n=U\cos\varepsilon+v\sin\varepsilon$ and this generates a force normal to the lifting line of $\mathrm{d}F=\rho u_n\Gamma\,\mathrm{d}s$. In the direction of the tethering lines, this force has a component $\mathrm{d}F\cos\theta$, so that the net line tension must be

$$2T=\rho\int\Gamma\cos\theta(U\cos\varepsilon+v\sin\varepsilon)\,\mathrm{d}s$$

and so, as required, the lift obtained using $L=2T\cos\varepsilon$ is consistent with the preceding result for the net lift.

The equations may now be simplified by using the sound approximation that $v\sin\varepsilon\ll U$. The natural reference length is the overall arc length $b$ of the lifting line and the natural area is the top surface area of the kite, $A$ (rather than the projected flying area); using $s=tb/2$ and forming coefficients using the reference force $\frac{1}{2}\rho AU^2$, the coefficients of tension, lift, and drag become

$$C_T=\frac{\cos\varepsilon}{2}\int_{-1}^{1}\frac{\Gamma b}{UA}\cos\theta\,\mathrm{d}t,\quad C_L=2\cos\varepsilon\,C_T \quad (3)$$

$$C_D=\int_{-1}^{1}\frac{\Gamma b}{UA}\left(\cos\theta\frac{v}{U}+\sin\theta\cos\varepsilon\frac{w}{U}\right)\mathrm{d}t=2\sin\varepsilon\,C_T \quad (4)$$

We may now pose the classical optimization problem of minimizing the drag subject to a constant value of the lift or, equivalently, minimizing $\varepsilon$ subject to a fixed tension. However, there is still a constraint to be added which arises from the local equilibrium of the kite forces. In the plane of the kite the force normal to the line $\mathrm{d}F$ must be resisted by the (constant) tension $T$ in the kite, requiring the kite curvature to be such that $T\,d\theta=\mathrm{d}F$. That is, by using the preceding results,

$$\frac{\mathrm{d}\theta}{\mathrm{d}t}=\frac{2\Gamma(t)}{\int_{-1}^{1}\Gamma\cos\theta\,\mathrm{d}t} \quad (5)$$

subject to the boundary conditions $\theta(0)=0$ and $\theta(1)=\theta_1$. In the case considered here where the length of the kite lines greatly exceeds the kite span, $\theta_1=\pi/2$.

These equations imply a structural model for the kite that allows no bending resistance about any axis normal to the kite plane but sufficient bending stiffness to resist any moment tending to deform the lifting line out of this plane. This in-plane bending stiffness also means that the tethering lines need not be attached at the base of the equivalent lifting line (e.g., at the quarter chord) but may be offset along the chord by the use of a bridle. This offset may then be used to counterbalance any residual overall $z$ moment in the kite, as given by

$$M_z=\int y(L\sin\varepsilon-D\cos\varepsilon)\,\mathrm{d}s=\int y(\sin\varepsilon\,\mathrm{d}L-\cos\varepsilon\,\mathrm{d}D)$$

removing any need to separately apply the requirement that this moment should vanish in the lifting-line model. It is in any case shown later that requiring $\sin\varepsilon\,\mathrm{d}L=\cos\varepsilon\,\mathrm{d}D$ at every point along the line leads to only a small change in the overall result, and so we can presume that enforcing the less restrictive overall requirement that $M_z$ should vanish would also produce only a small change.

## Aerodynamic Forces and Kite Shape Under a Given Loading

The solution proceeds best by making the usual transformation to $t=\cos\phi$ and writing the loading as a series with the correct end conditions:

$$\frac{\Gamma}{Ub}=\frac{1}{2}\sum_{n=1}^{\infty}A_n\sin n\phi$$

The strength of the vortex sheet shed into the wake may then be found from the loading using the standard result[16]:

$$\frac{\gamma}{U}=\frac{1}{U}\frac{\mathrm{d}\Gamma}{\mathrm{d}s}=-\sum_{n=1}^{\infty}nA_n\frac{\cos n\phi}{\sin\phi} \quad (6)$$

Writing

$$A_T=\frac{1}{2}\sum_{n=1}^{\infty}A_n\int_0^{\pi}\cos\theta\sin\phi\sin n\phi\,\mathrm{d}\phi=\frac{2C_T}{\Lambda\cos\varepsilon}$$

string equation (5) then conveniently becomes

$$A_T\frac{\mathrm{d}\theta}{\mathrm{d}\phi}=-\sum_{n=1}^{\infty}A_n\sin\phi\sin n\phi$$

$$=\sum_{n=1}^{\infty}\frac{A_n}{2}[\cos(n+1)\phi-\cos(n-1)\phi]$$

in which $A_T$ is an unknown constant. This equation can be integrated exactly.

Taking only odd values of $n$ so that the loading is symmetric, the requirement of zero slope at the center ($\phi=\pi/2$) is satisfied if $A_T=\frac{1}{2}A_1$ when

$$\theta=\frac{\pi}{2}-\phi+\frac{\sin2\phi}{2}+\sum_{n=3}^{\infty}\frac{A_n}{A_1}\left[\frac{\sin(n+1)\phi}{n+1}-\frac{\sin(n-1)\phi}{n-1}\right] \quad (7)$$

Note that the result for $A_T$ means that $C_L=2\cos\varepsilon C_T=\frac{1}{2}A_1\Lambda\cos^2\varepsilon$ and so the tension and lift still depend only on the first term in the loading, for any kite shape.

The calculation of the drag is greatly simplified by employing the assumption that $\varepsilon$ is small, which is in any case consistent with this small-disturbance theory, so that the inclination of the kite plane may be ignored and the induced angles can be found by assuming that the wake is semi-infinite from the $y$–$z$ plane. This assumption is therefore employed in the remaining analysis. The induced velocities in the expression for drag then combine to represent the net flow normal to the lifting line in this plane. At an arc length $s_o$, this may be written in the form

$$v_n(s_o)=\frac{1}{4\pi}\int_{-b/2}^{b/2}\frac{\cos[\alpha(s,s_o)-\theta(s_o)]}{r(s,s_o)}\gamma(s)\,\mathrm{d}s$$

$$=\frac{1}{4\pi}\int_{-b/2}^{b/2}\frac{g(s,s_o)}{(s-s_o)}\gamma(s)\,\mathrm{d}s$$

where $\tan\alpha=-(z-z_o)/(y-y_o)$, and $r$ is the linear distance between the two points $(y,z)$ and $(y_o,z_o)$ represented by $s$ and $s_o$ on the arc. Because the function $g$ may then be seen to be a regular function of the lifting-line geometry, this is in a form allowing Gaussian integration using Lan's method,[17] whereby the integral may be represented at certain specific control points by an equivalent system of vortices placed at certain specific vortex points. The result is exact if for each $s_o$ the product $\gamma g$ is a polynomial in $s$ to a certain order. For $N$ vortex points, the speed at each control point $s_k$ ($k=1,N$) is then

$$v_n(s_k)=\sum_{i=1}^{N}\frac{W_i\gamma(s_i)}{r(s_k,s_i)}\cos[\alpha(s_k,s_i)-\theta(s_k)] \quad (8)$$

where $s_k = -\cos(k/N)\pi$, $s_i = -\cos[(2i-1)/2N]\pi$, and $W_i = \sin\phi_i/4N$.

If the loading terms $A_n$ are all specified, then the kite line shape may be found simply by using Eq. (7) and integrating $dx = \cos(\theta)\,ds$, $dy = \sin(\theta)\,ds$. The normal speeds at the control points may then be found by using Eq. (8), enabling the drag coefficient to be evaluated from Eq. (4) by changing the integration variable to $\phi$ and using the midpoint approximation.

The accuracy of this numerical method is demonstrated here in two steps. First, the wing shape was assumed to be semicircular and the nonzero terms in the loading were given typical proportions with $A_1 = 1.0$, $A_3 = -0.1$. The induced speed normal to the lifting line was calculated using Eq. (8) at five control points along one side of the arc, along with the overall drag coefficient, first with 10 vortex points on each side and then with 5. It was found that the induced angle $v_n/U$ varied by less than 0.001 between these two cases, and the drag by less than 0.3%. The arc shape was calculated next according to the aforementioned theory, keeping the loading the same and representing the kite shape by $2N$ linear segments on each side and $N$ control point ($N = 5$, 10, 20). The resulting values for the $x$ coordinate of the tips of the lifting line, the induced normal speed at the center of the lifting line, and the overall drag coefficient were all plotted against $1/N$. A straight line was fitted to each dataset to confirm that this is the expected convergence rate with $N$, and by extrapolation it was found that in each case the results with $N = 20$ were within less than 0.3% of the result for $N = \infty$. Because $N = 20$ is used in the following analysis, this is the expected accuracy of all the quoted results.

## Optimal Shapes

If the lifting line remains straight the usual lifting-line result for the drag will be obtained: $C_D = nA_n^2/\pi$. It is well known that the optimum loading is thereby elliptic (that is, only $A_1$ is nonzero), and so the drag angle would be given by $\varepsilon = 2A_1/\Lambda\pi$. This loading produces a constant downwash on a straight lifting line but not on a curved one. In the general case if $\int \Gamma\cos\theta\,ds$ is to be fixed and $\int \Gamma v_n\,ds$ to be at a minimum, as Eqs. (3) and (4) imply, then both integrals must remain constant for small variations in loading. For arbitrary variations this can only be true if the normal speed $v_n$ is everywhere proportional to $\cos\theta$, and this well-known result is often used as an alternative way of finding the optimum loading. However, it cannot apply to the present problem, because small variations in loading will also produce variations in shape; that is, the distribution of $\theta$ is not known a priori. Note that if the two integrands of Eq. (2) were required to balance at *every* value of $s$, then, with $\varepsilon \ll 1$, we would indeed obtain $v_n = U\sin\varepsilon\cos\theta$. However, this constraint is stronger than needed, and so the loading derived from it is not the optimum.

The general result must be obtained instead by fixing $A_1$ and choosing the remaining $A_n$ of a truncated series to minimize $C_D$. Here the first 10 terms were used (odd values of $n$ only) and the associated induced angles and arc shape have been found using the preceding method. The values of $A_n$ required to minimize drag for a given lift were found using the Newton optimizer provided in Excel. To check the optimization routine the optimal loading was first found for a semicircular wing, when the efficiency based on the flying span was found to be 1.5005 compared with the theoretical value[7] of 1.5000.

The results for the optimal kite loading are given in Table 1, where it may be seen that $A_n$ diminish rapidly with $n$, so that no more than three or four terms are required. (In fact if only two terms are used the values quoted in the following change by less than 0.1%.) The resulting wing shape and loading are shown in Figs. 3a and 3b, where the flying span is 54% of the actual span and the kite height 35%. The

**Table 1 Terms in the loading series, as a ratio to the first term**

| $k_0$ | $k_2$ | $A_3/A_1$ | $A_5/A_1$ | $A_7/A_1$ | $A_9/A_1$ |
|---|---|---|---|---|---|
| 0.0 | 0.0 | −0.0329 | 0.0037 | −0.0003 | 0.0000 |
| 0.05 | 0.03 | 0.02135 | 0.00742 | 0.00118 | 0.00047 |

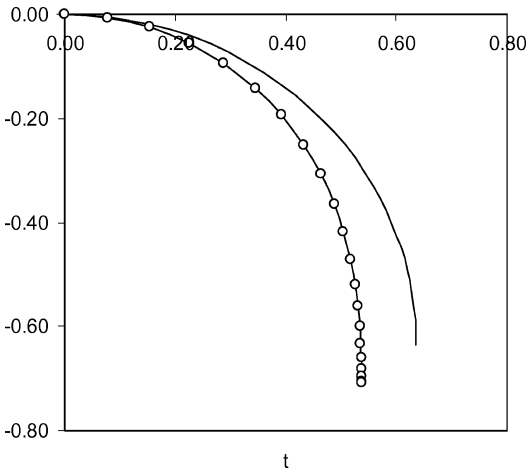


**Fig. 3a Shape of the optimal kite in inviscid flow (○, kite shape and ——, reference semicircle).**

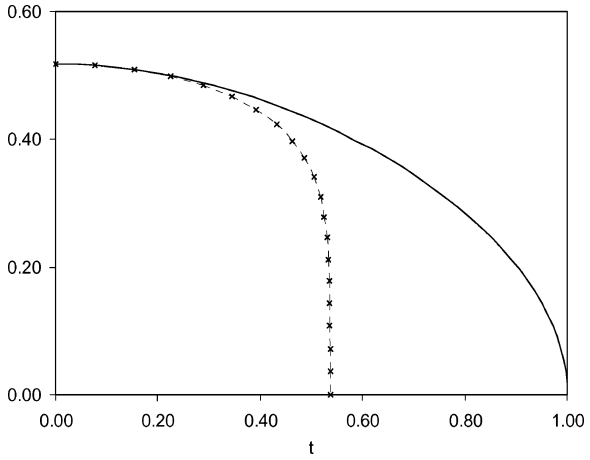


**Fig. 3b Shape of the optimal loading (——, kite loading vs span and ×, kite loading projected vertically onto the kite).**

drag is $C_D = 0.662C_L^2/\Lambda$ so that the drag angle is $\varepsilon = 0.662C_L/\Lambda$ and the wing efficiency is 0.481. It should be noted that, because a lifting line has no reference area other than $b^2$, at this stage the effect of aspect ratio on these results is artificial: if $b^2$ is used to define the reference area, then the aspect ratio disappears from all of the preceding analysis. However, the drag angle increases with lift coefficient, because the drag increases with the square of the lift.

To compare the optimal kite with a semicircular wing, the efficiency must be based on the arc length in each case rather than the tip-to-tip flying span, which is usually used, when the result for a semicircle becomes 0.607. This is much better than that of the kite simply because its profile is much flatter (as shown in Fig. 3a) so that a given loading will generate more lift but a similar drag. If the kite shape is then held fixed in the optimal shape and the loading is readjusted so that the drag is minimized without the constraint of cable equation (4), then the efficiency rises to 0.50 and the required normal velocity is indeed found to be a constant as required by the variational argument given earlier: $v_n = 0.33A_1\cos\theta$. If instead the condition $v_n = U\cos\theta$ is enforced at *every* point on the flexible kite, as discussed earlier, the efficiency is 0.46 and the drag angle rises to $0.69C_L/\Lambda$. Although these differences are quite small, the relative performance of each of these cases is consistent with the preceding arguments; that is, as more restrictive constraints are added, the performance drops. The results of Table 1 also show that the optimal loading is quite close to elliptic, which raises the question of what happens if the loading is not optimal. If the loading is exactly elliptic, the efficiency drops only slightly to 0.48. However, if we take $A_3 = 0.1A_1$, which quite significantly flattens the loading profile, the efficiency falls by about 5%.

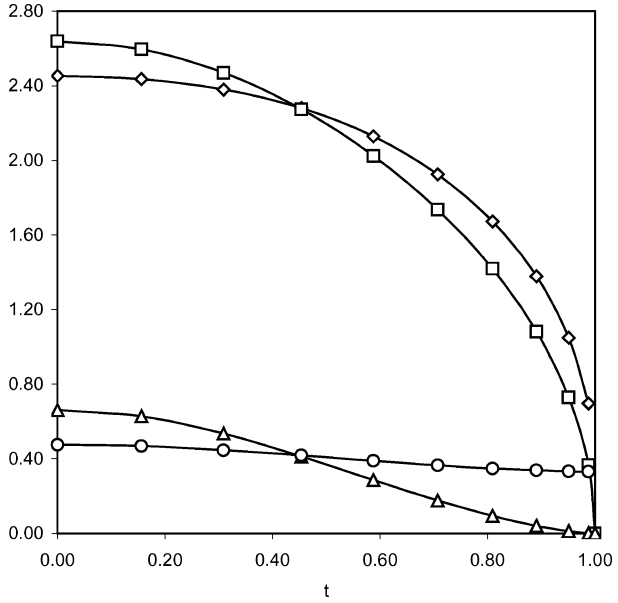


**Fig. 4 Angles needed for optimum loading (as a ratio to $C_L/\Lambda$) for a kite of constant chord and aspect ratio 8, with no profile drag (□, $\alpha_{\text{eff}}$; ○, $\alpha_i$; ◇, $\alpha_t$; and △, $\alpha_k$).**

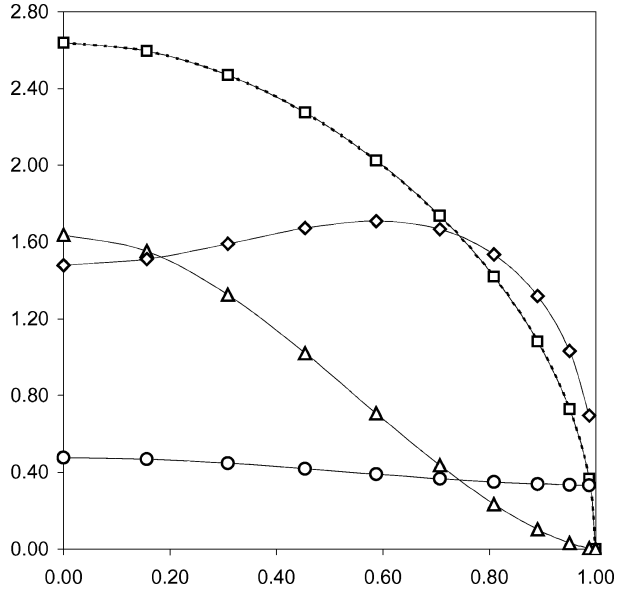


**Fig. 5 Angles needed for optimum loading (as a ratio to $C_L/\Lambda$) for a kite of constant chord and aspect ratio 8, with constant profile drag added (□, $\alpha_{\text{eff}}$; ○, $\alpha_i$; ◇, $\alpha_t$; and △, $\alpha_k$).**

For design purposes it is also helpful to know the distribution of sectional lift and twist corresponding to the optimal loading, and these may be found in the usual way. For a chord distribution $c(s)$, the sectional lift coefficient is

$$c_l(s) = [2\Gamma(s)/bU][b/c(s)] = 2\pi\alpha_{\text{eff}} = 2\pi(\alpha_g - \alpha_i) \qquad (9)$$

where $\alpha_{\text{eff}}$ is the effective angle of attack needed, $\alpha_g$ is the geometric angle of attack, and the induced angle $\alpha_i$ is $v_n/U$. Note that the associated sectional lift force is not vertical but lies in the kite plane and normal to it. The induced angle required to achieve the optimum loading is shown in Fig. 4. The geometric angle is made up partly of the angle of attack due to the inclination of the kite plan, $\alpha_k = \varepsilon\cos\theta$, and partly of the twist $\alpha_t$ needed in the kite section along its span (as a rotation from the zero-lift angle about the lifting line).

From the results just presented, all of these angles are proportional to $C_L$, but because $\alpha_{\text{eff}}$ is also proportional to the aspect ratio the twist must depend on both. The variation of each of these angles is illustrated in Fig. 4 for a kite of constant chord and an aspect ratio of 8, from which the distribution needed for other shapes may be deduced. If the kite shape is tapered toward the tip, for example, the effective angle becomes more uniform but the twist variation increases.

Thus far the analysis has excluded any effects of viscosity, but these may be readily accomodated by incorporating a sectional profile drag coefficient based on the local chord, the usual form being $c_d = k_0 + k_1 c_l + k_2 c_l^2$. The viscous drag may then be integrated up and added to the induced drag, and the total minimized as before by adjusting the loading. Now, of course, the results will vary with aspect ratio, planform, and lift coefficient, but they are given here only for the constant-chord wing used earlier. The lift coefficient is $C_L = 0.64$, or about the highest value that might be expected in practice, with an aspect ratio of 8. From the preceding results, the optimal kite in inviscid flow then has $C_D = 0.0339$ and $\varepsilon = 3.0$ deg.

Experimental data for the drag of two-dimensional single-surface membranes covers a wide range (Jackson[18] quotes 0.015 to 0.05), and data for double surface sections are equally uncertain. Karn's experiments[19] on fully and partially double-surface wings formed by wrapping membrane around a spar found drag coefficients in the range 0.03 to 0.10 at Reynolds numbers around $2 \times 10^5$, depending on the slackness ratio (or camber) of the membrane. Although much might be learned from studies of parafoils, most have been aimed at finding the overall lift and drag coefficients rather than the sectional characteristics (see, for example, Ref. 20). Given the uncertainty in these data, results will be presented here for a range of likely values.

Results are shown first using a constant profile drag: $k_0 = 0.05$, $k_1 = 0.00$, $k_2 = 0.00$. As expected this makes no difference to the optimum loading and so the induced drag remains at 0.0338 but the total rises to 0.0838 and the flying angle to 7.5 deg. because the loading is the same as before, the distributions of the effective and induced angles are unchanged, but because the flying angle has increased so has the inclination angle of the kite, $\alpha_k$, and therefore the twist needed to maintain the same loading is dramatically different, as shown in Fig. 5. Corresponding results for other values of profile drag $k_0$ may be deduced from these curves.

Finally, results are shown with lift-dependent profile drag added: $k_0 = 0.05$, $k_1 = 0.00$, $k_2 = 0.03$. Because this now penalizes areas of high sectional lift, the optimum loading is flatter than before, with the coefficients as given in Table 1. The induced drag rises slightly to 0.0342 and the profile drag rises to 0.0824, giving an overall flying angle of 10.4 deg. The distributions of the various angles are shown in Fig. 6. Because the chord is constant, the shape of $\alpha_{\text{eff}}$ reflects that of the new loading, with the distribution for the previous effective angle being shown for comparison. Because the loading has changed shape only slightly, the distribution of the induced angle $\alpha_i$ is not much different than before. However, because the drag angle has increased again, the necessary twist needed to be built into the kite has again changed markedly.

By reworking the analysis for this planform with other values for the terms in the profile drag, a general expression for drag was found to be

$$C_D = k_0 + 2.6k_2C_L^2 + C_L^2/0.47\pi\Lambda \qquad (10)$$

Because the flying angle is determined by the drag/lift ratio, it is clear that for a given kite planform the best performance will now be obtained at a particular lift coefficient, in this case that which makes the lift-dependent drag exactly half of the total; that is, when

$$C_L = \sqrt{\frac{k_0\Lambda}{2.6\Lambda k_2 + 0.68}}$$

For example, with the values used previously for $k_0$ and $k_2$, this gives $C_L = 0.55$ and $C_D = 0.10$ with a flying angle of $\varepsilon = 10.2$ deg. In practice the aerodynamic drag must also include that of the kite lines and of the vehicle being drawn, and because these are blunt bodies this parasite drag can be very significant and must be added to $k_0$.

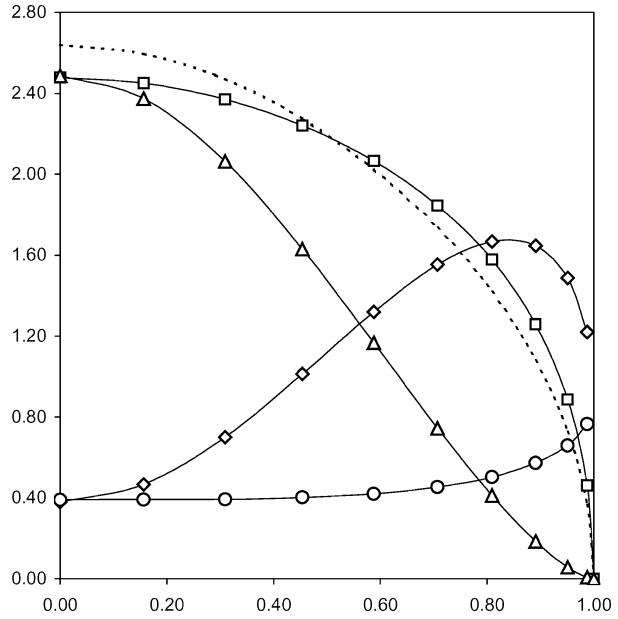


**Fig. 6 Angles needed for optimum loading (as a ratio to $C_L/\Lambda$) for a kite of constant chord and aspect ratio 8, with lift-dependent profile drag added (□, $\alpha_{\text{eff}}$; ○, $\alpha_i$; ◇, $\alpha_t$; and △, $\alpha_k$; dashed line shows the ideal effective angle from Fig. 5).**

Finally, it is postulated that this lifting-line model may also explain why these kites naturally tend to align themselves normal to the wind. The Kutta–Joukowski forces acting near the ends of the kite are directed horizontally and normal to the wind, so that if the kite yaws about a vertical axis these forces provide a restoring moment that turns it back again. We may presume that the same forces are responsible for the deliberate turning of a kite by means of the control lines. If the kite is "rolled" by pulling down on one line, the net lift force must rotate toward that side, causing the kite to begin moving sideways in that direction. This adds a component of incident wind so that apparent wind comes from the side to which the kite is swaying, and the action of the forces described earlier turns the kite to face the same way.

## Conclusions

The use of a tensioned lifting line has provided some useful results for the minimum induced drag on a tension kite along with the distributions for the associated loading and the effective and induced angles. As with any other kind of wing, there are many different planform and twist distributions that can produce the necessary loading, and these may be derived from the results given here for the associated angles. Of course in practice the practicable shapes will be constrained by the ability of the kite to resist torsion and this in turn depends on details of construction and equilibrium which cannot be modeled with a tensioned lifting line.

The theory shows that the loading which produces the minimum induced drag on a tension kite is quite close to elliptic loading and has an efficiency of 48%, based on the true kite span, and that for nonoptimal shapes the efficiency is still likely to be about 45%. Based on the projected flying area the best efficiency is 167%, which compares favorably with the 150% achieved by a semicircular wing. With no profile drag, the flying angle increases with the lift coefficient, so that lightly loaded kites will perform best in this respect.

The inclusion of profile drag means that the flying angle of the kite must change, and this in turn alters the effective angle of attack along the whole kite span. We therefore have the very unusual situation where the aerodynamics of this lifting surface may not be approximated by ignoring viscous effects: there is a first-order interaction between the two. Although the efficiency is poor, even for the optimal kite shape, and so the induced drag is higher than normal for a given lift coefficient, the smoothness of the inflated membrane section is likely to be even worse than usual so that the profile drag will be at least as great as the induced drag. This means that the practical application of this theory will require experimental determination of better data on the profile drag for sections of this kind.

## Acknowledgment

The author thanks Jeremy Pilkington, Flexifoil International, Ltd., for the use of the photograph in Fig. 1.

## References

[1]Alexander, K., and Stevenson, J., "Kite Equilibrium and Bridle Length," *Aeronautical Journal*, Vol. 105, No. 1051, 2001, pp. 535–541.

[2]Newman, B. G., "Aerodynamic Theory for Membranes and Sails," *Progress in Aerospace Sciences*, Vol. 24, No. 1, 1987, pp. 1–27.

[3]Smith, R., and Shyy, W., "Computational Model of Flexible Membrane Wings in Steady Laminar Flow," *AIAA Journal*, Vol. 33, No. 10, 1995, pp. 1769–1777.

[4]Jackson, P. S., and Fiddes, S. P., "Two-Dimensional Viscous Flow past Flexible Sail Sections Close to Ideal Incidence," *Aeronautical Journal*, Vol. 99, No. 986, 1995, pp. 217–225.

[5]Boudreault, R., "3-D Program Predicting the Flexible Membrane Wings Aerodynamic Properties," *Journal of Wind Engineering and Industrial Aerodynamics*, Vol. 19, Nos. 1–3, 1985, pp. 277–283.

[6]Ormiston, R. A., "Theoretical and Experimental Aerodynamics of the Sailwing," *Journal of Aircraft*, Vol. 8, No. 2, 1971, pp. 77–84.

[7]Murai, H., and Maruyama, S., "Theoretical Investigation of Sailwing Airfoils Taking Account of Elasticities," *Journal of Aircraft*, Vol. 19, No. 5, 1982, pp. 385–389.

[8]Nickel, K. L. E., "Theory of Sail-Wings," *Zeitschrift fuer Flugwissenschaften und Weltraumforschung*, Vol. 11, No. 6, 1987, pp. 321–328.

[9]Sneyd, A. D., "Aerodynamic Coefficients and Longitudinal Stability of Sail Aerofoils," *Journal of Fluid Mechanics*, Vol. 149, 1984, pp. 127–146.

[10]Holla, V. S., Rao, K. P., Asthana, C. B., and Arokkiaswamy, A., "Aerodynamic Characteristics of Pretensioned Elastic Membrane Rectangular Sailwings," *Computer Methods in Applied Mechanics and Engineering*, Vol. 44, No. 1, 1984, pp. 1–16.

[11]Sugimoto, T., "Analysis of Circular Elastic Membrane Wings," *Transactions of the Japanese Society of Aerodynamics and Space Sciences*, Vol. 34, No. 105, 1991, pp. 154–166.

[12]Letcher, J. S., "Membrane Theories for 3-Dimensional Inextensible Sails," *16th Symposium on the Aero/Hydronautics of Sailing*, AIAA/SNAME, Los Angeles, 1986, pp. 120–128.

[13]Sugimoto, T., "A Theory for Inextensible and High Aspect-Ratio Sails," *Journal of Wind Engineeering and Industrial Aerodynamics*, Vol. 63, Nos. 1–3, 1996, pp. 61–75.

[14]Jackson, P. S., "Theory for Conical Membrane Wings of High Aspect Ratio," *AIAA Journal*, Vol. 39, No. 5, 2001, pp. 781–786.

[15]Marchaj, C. A., *Aero-Hydrodynamics of Sailing*, Granada, London, 1979.

[16]Bertin, J. J., and Smith, M. L., *Aerodynamics for Engineers*, Prentice–Hall International, London, 1989.

[17]Lan, E. C., "A Quasi-Vortex Lattice Method in Thin Wing Theory," *Journal of Aircraft*, Vol. 11, No. 9, 1974, pp. 518–527.

[18]Jackson, P. S., "Theory for Conical Membrane Wings of High Aspect Ratio," *AIAA Journal*, Vol. 39, No. 5, 2001, pp. 781–786.

[19]Karn, R., "Experimental Study on Inflated Double Surface Sails," Mechanical Engineering, Univ. of Auckland, Auckland, New Zealand, 1982.

[20]Matos, C., Mahalingam, R., Ottinger, G., Klapper, J., Funk, R., and Komerath, N., "Wind Tunnel Measurements of Parafoil Geometry and Aerodynamics," AIAA Paper 98-0606, Jan. 1998.

A. Plotkin
*Associate Editor*